materials

MDPI

Article

Facile Fabrication of Dumbbell-Like β-Bi_2O_3/Graphene Nanocomposites and Their Highly Efficient Photocatalytic Activity

Jun Yang [1,†], Taiping Xie [2,*,†], Chenglun Liu [3,4] and Longjun Xu [3,*]

1 Chongqing Key Laboratory of Environmental Materials & Remediation Technologies, Chongqing University of Arts and Sciences, Yongchuan 402160, China; bbyangjun@foxmail.com
2 Chongqing Key Laboratory of Extraordinary Bond Engineering and Advanced Materials Technology (EBEAM), Yangtze Normal University, Chongqing 408100, China
3 State Key Laboratory of Coal Mine Disaster Dynamics and Control, Chongqing University, Chongqing 400044, China; xlclj@cqu.edu.cn
4 College of Chemistry and Chemical Engineering, Chongqing University, Chongqing 401331, China
* Correspondence: deartaiping@163.com(T.X.); xulj@xqu.edu.cn (L.X.)
† The two authors contributed equally to this work.

Received: 10 July 2018; Accepted: 3 August 2018; Published: 6 August 2018

Abstract: β-Bi_2O_3 decorated graphene nanosheets (β-Bi_2O_3/GN) were prepared by a facile solution mixing method. The crystal structure, surface morphology, and photo absorbance properties of the products were characterized by XRD, SEM, and UV-VIS diffuse reflection, respectively. Moreover, the effect of graphene content on photocatalytic activity was systematically investigated, and the results indicated that these composites possessed a high degradation rate of Rhodamine B (RhB), which was three times higher than that of bare β-Bi_2O_3 when graphene content was 1 wt %. This high photocatalytic activity was attributed predominantly to the presence of graphene, which served as an electron collector and transporter to efficiently lengthen the lifetime of the photogenerated charge carriers from β-Bi_2O_3.

Keywords: Dumbbell-like β-Bi_2O_3; photocatalysis; β-Bi_2O_3/GN; graphene-based composite

1. Introduction

The semiconductor can be used as a photocatalyst due to its unique electronic component structure (a valence band full of electrons and an empty conduction band). Bi_2O_3 is a common important semiconductor material, which is widely used in various fields, such as electronic ceramics, sensors, and high-temperature superconductivity, to name a few [1,2]. As a photocatalyst, it has gained more and more attention [3]. Bi_2O_3 mainly has four crystal structures, including α, β, γ, and δ. Due to a lower band gap and a unique electronic structure, the β-Bi_2O_3 has higher photocatalytic activity than the other configurations of Bi_2O_3 [4,5]. However, the photocatalytic activity of pure Bi_2O_3 is still restricted. In order to further enhance its activity, researchers have made efforts, such as using Pt, Au, Ag, and other noble metals, to improve the conductivity of the electrons and reduce the recombination probability of charge carrier [6,7]. Chai et al. [8] used Bi_2O_3 as a precursor to prepare the BiOCl/Bi_2O_3 complex and finally form a heterojunction so as to significantly improve its activity in the photocatalytic degradation of pollutants.

In recent years, graphene-based semiconductor photocatalysts have gained great attention due to their highly efficient electronic conduction force, larger specific surface area, and good adsorption performance [9]. To date, various graphene–semiconductor composites with enhanced photocatalytic performance have been designed, such as graphene–TiO_2 nanocomposite [10], graphene/zirconium

oxide [11] and RGO–Bi_2O_3 nanocomposite [12]. As far as we know, only a few research studies with graphene-based Bi_2O_3 used as a photocatalyst have been reported. For example, Som et al. [13] and Maruthamani et al. [14] introduced a co-precipitation route to prepare GO/α-Bi_2O_3 or rGO/Bi_2O_3 rods. Cao et al. [15] explored an organic electrolyte-assisted method to prepare the GR/β-Bi_2O_3 composites. Therefore, in this paper, we consider it important to undertake the green chemical synthesis of the composites; a simple method of solution mixing and thermal reduction was used to prepare β-Bi_2O_3 decorated graphene nanosheets (β-Bi_2O_3/GN) in one step. Rhodamine B (RhB) is used as the model organic dye to investigate the activity of as prepared samples, as it is an important factor in environmental pollution and its degradation mechanism has been studied quite well [16,17]. In addition, the effect of the content of graphene was also studied systematically, and finally, a possible photocatalytic mechanism of β-Bi_2O_3/GN composite was proposed.

2. Experimental

2.1. Synthesis of Bi_2O_3/GN

Graphite oxide was prepared by a modified Hummers method [18]; then, the aqueous solution of graphene oxide (GO) could be obtained by ultrasonic stripping from graphite oxide for 1 h. β-Bi_2O_3-decorated graphene nanosheets (β-Bi_2O_3/GN) were prepared by a facile solution mixing method and thermal reduction. In a typical process, 8 mmol of $Bi(NO_3)_3 \cdot 5H_2O$ was dissolved in 20 cm^3 of nitric acid (1 mol/dm^3); then, a different volume of GO (2 mg/dm^3) was added dropwise into the solution, which was then continuously stirred for 30 min. Then, the above solution was added dropwise into 80 cm^3 (0.6 mol/dm^3) of saturated sodium carbonate solution. The reaction mixture was stirred for 5 h before filtration. After being washed by water and ethanol several times respectively, the whole product was dried at 60 °C for 10 h. The dried product was then transferred into the muffle furnace after being ground. Finally, the dried product was roasted at 360 °C for 10 min under the nitrogen atmosphere protection, then, it was natural cooled to room temperature to obtain the resultant product. Here, it was worth noting that the heating rate was 4 °C/min. During the reaction, GO was reduced to GN. Pure β-Bi_2O_3 was synthesized by the same experimental process, except that GO was not added.

2.2. Materials' Characterization

The samples' crystal structure was characterized by XRD (Bruker Advance D8, Cu Kα irradiation, Bruker, Germany). Scanning electron microscopy (SEM, JSM-7800F, Japan electronics, Japan) was used to observe the morphology of the prepared samples. The Fourier transform infrared spectroscopy (FTIR) spectra of samples were recorded on a 5DX FTIR (5DX, Nicolet. Co., Rhinelander, WI, USA) spectrometer using KBr powder-pressed pellets. The Brunauer–Emmett–Teller (BET) special surface area was determined through N_2 adsorption at 77 K using an adsorption instrument (ASAP-2020, Micromeritics, Norcross, GA, USA). The UV-VIS diffuse reflectance spectra (UV-vis DRS) of samples were measured using a UV-VIS spectrophotometer (TU1901, Beijing Purkinje, Beijing, China).

2.3. Test of Photocatalytic Activity

The photodegradation test was carried out by using a 300-W xenon lamp (the corresponding emission spectrum see Figure S1) (CEL-HXF300, AULTT, Beijing, Country), the self-made circulating water system maintained the temperature of the reaction system at 25 ± 5 °C. RhB solution (50 cm^3, 10 mg/dm^3) containing 50 mg of catalyst was put in a glass beaker and stirred in the dark overnight to ensure adsorption–desorption equilibrium. After light illumination at regular time intervals, the absorbance of the RhB solution was monitored by a UV-VIS spectrophotometer.

3. Results and Discussion

3.1. Crystal Structure Characterization

Figure 1 shows the XRD patterns of pure β-Bi_2O_3 and composites with different masses of GN. The peak positions of 27.9°, 31.7°, 32.6°, and 33.8° correspond to the crystal plane diffractions of (201), (002), (220), and (102) of the tetragonal β-Bi_2O_3 (JCPDS 27-0050), respectively. The diffraction peaks of the β-Bi_2O_3/GN sample and β-Bi_2O_3 are essentially the same, except for a few diffraction peaks of $Bi_2O_2CO_3$ (the inverted triangle as shown in Figure 1. This may be due to the coating effect of GN, which caused $Bi_2O_2CO_3$ to not be completely converted into β-Bi_2O_3 in the thermal decomposition process. However, $Bi_2O_2CO_3$ has a similar electronic structure to Bi_2O_3, which is also a well-known photocatalyst. When $Bi_2O_2CO_3$ was used as the photocatalytic material, it can play a synergistic effect. For example, Chai et al. reported that one β-Bi_2O_3/$Bi_2O_2CO_3$ nanosheet composite exhibits much higher photodegradation activity than single phase [5]. It was worth noting that there were no significant carbon-related diffraction peaks in XRD, which is because of the low GN content and low diffraction intensity [19].

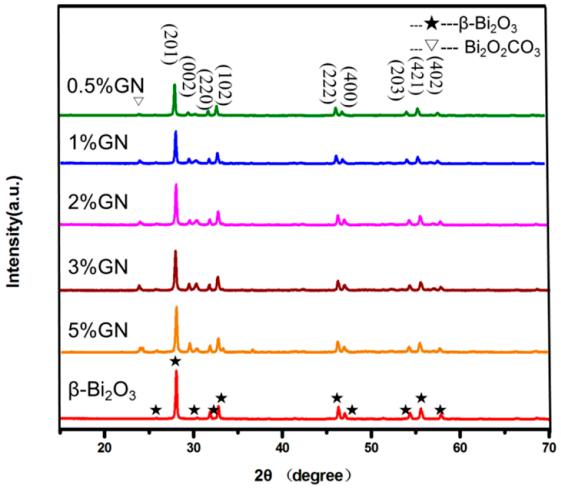

Figure 1. Diffraction patterns of pure β-Bi_2O_3 and hybrid composites with different mass ratios of graphene nanosheets (GN).

3.2. FTIR Spectra

In order to better analyze the state of GN on the surface of β-Bi_2O_3, the FTIR of β-Bi_2O_3/GN (1%) and β-Bi_2O_3/GO are displayed in Figure 2. It can be seen that the composites both have a peak at 500–700 cm^{-1}, which belongs to the telescopic vibration of the Bi–O bond of BiO_6 octahedron, and the telescopic vibration peak at 840 cm^{-1} belongs to Bi–O–Bi [20]. In addition, the O–H stretching vibration of adsorbed water corresponds to 3450 cm^{-1}, and the O–H stretching vibration peak in C–O–H corresponds to 1408 cm^{-1} [21,22]. The peaks at 1440–1630 cm^{-1} can be attributed to the antisymmetric stretching vibration and symmetry stretching vibration of the C=O bond in –COOH, respectively. It is worth noting that the C=O antisymmetric stretching vibration at 1450 cm^{-1} has disappeared after the thermal reduction, and what's more, the peak intensity becomes weaker after reduction, indicating the effectiveness of the thermal reduction. The results of FTIR show the existence of GO and Bi_2O_3 in the composites, and GO is effectively reduced to GN after thermal reduction.

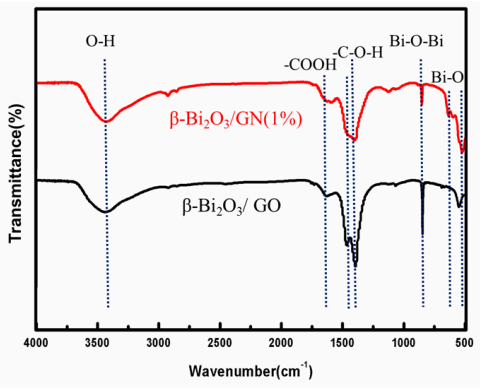

Figure 2. Fourier transform infrared (FTIR) spectra of β-Bi_2O_3/GN (1%) and β-Bi_2O_3/GO.

3.3. Surface Morphology Characterization

Surface morphology of the samples was characterized by SEM (Figure 3). The pure β-Bi_2O_3 is as shown in Figure 3a. β-Bi_2O_3 has a dumbbell-like morphology (the insert is dumbbell). After the 1% GN was introduced, it can be clearly seen that the β-Bi_2O_3 was coated by GN (Figure 3b) or embedded in the GN sheets (Figure 3c). In Figure 3b, it can also be seen there is very little $Bi_2O_2CO_3$, which was consistent with the XRD results. The elemental mapping (Figure 3d) of the ternary as-prepared β-Bi_2O_3/GN obtained by EDS (the mapped region highlighted with red frame in Figure 3b) indicates that the weight ratios of the elements are close to the Bi_2O_3 molar mass ratios. Meanwhile, only the peaks of C, O, Bi, Au were detected, which means that the as-prepared composites are composed of graphene and Bi_2O_3.

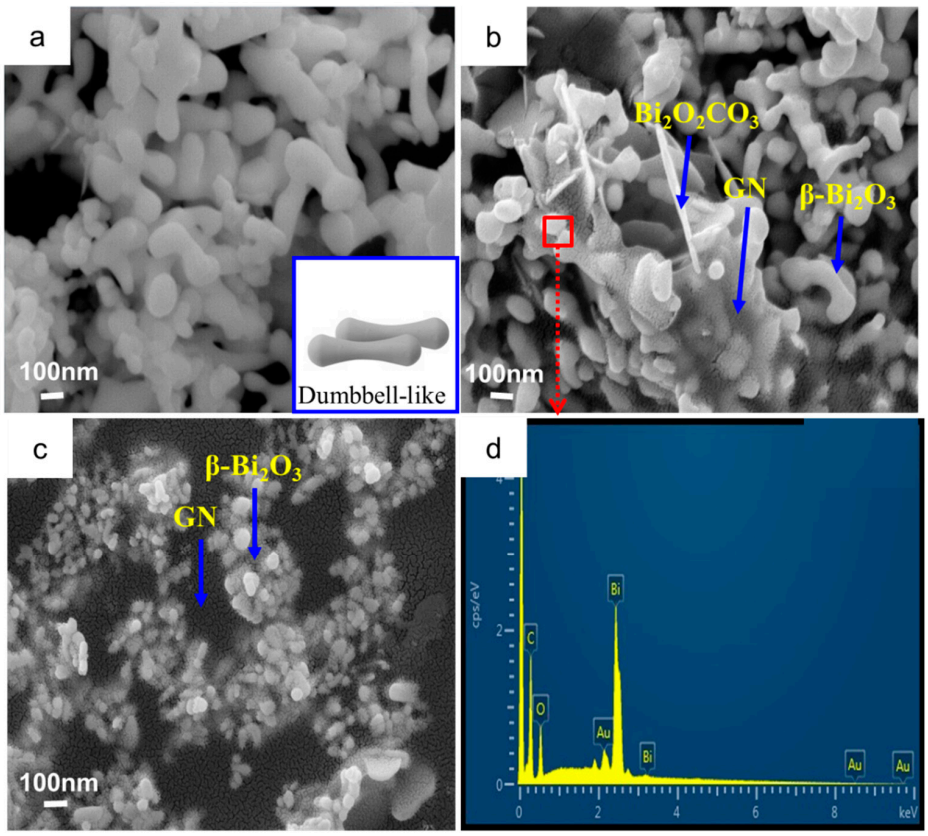

Figure 3. (**a**) SEM images of pure β-Bi_2O_3; (**b**,**c**) β-Bi_2O_3/GN(1%); and (**d**) EDS pattern of β-Bi_2O_3/GN.

3.4. Surface Areas and Pore Size Distributions

In general, the specific surface area of catalysts and its surface structure have significant influences on catalytic activity. Therefore, the specific surface analyzer is utilized to implement further research on the specific surface area and the pore diameter distribution of pure β-Bi_2O_3 and β-Bi_2O_3/GN (1%). Figure 4 shows the N_2 adsorption–desorption isotherms and the corresponding curves of the pore size distribution (inset) for samples β-Bi_2O_3 and β-Bi_2O_3/GN (1%). According to the Brunauer–Deming–Deming–Teller (BDDT) classification, pure β-Bi_2O_3 isotherms can be categorized as type III (Figure 4a), which is convex to the P/P_0 axis over its entire range, indicating that the pure β-Bi_2O_3 belong to a nonporous structure. Meanwhile, samples of β-Bi_2O_3/GN (1%) have isotherms of type IV, suggesting the presence of mesopores. Upon observing the pore diameter distribution diagram obtained from desorption isotherms, pore diameter mainly distributes in 5.28 nm (Figure 4b inset). The specific surface area of β-Bi_2O_3 and β-Bi_2O_3/GN (1%) are given by BET measurement as 3.37 m^2/g, 4.53 m^2/g, respectively, which conforms to the results. In other words, when graphene is introduced, mesopores begin to appear in samples and the specific surface area increases, which is because the prepared nanocomposite is composed of sheet-like graphene decorated with β-Bi_2O_3, similar to the previous report [23]. Consequently, the introduction of graphene can increase the specific surface area, and graphene may play a role in enhancing the photocatalytic activity.

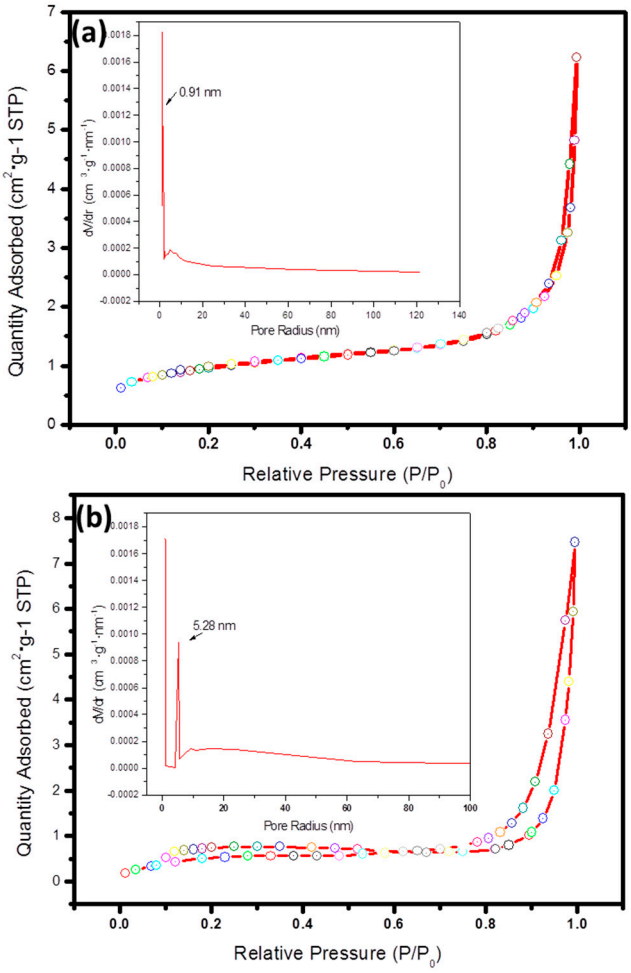

Figure 4. N_2 adsorption–desorption isotherm of (**a**) β-Bi_2O_3 and (**b**) β-Bi_2O_3/GN (1%). Inset: the corresponding pore size distribution.

3.5. UV-Vis Diffuse Reflectance and Photocatalytic Activity

The photocatalytic activity tests are shown in Figure 5. From Figure 5a, the absorption of visible light by the samples can be seen as the content of GN increases, and the sample color gradually changing from yellow to deeper brown can also be seen in Figure 5c. This is another proof to the increasing absorption of visible light. The band gap of calculated β-Bi_2O_3 and composites are shown in Figure 5b. Although the 5% GN is not narrowest band gap, the absorbed threshold value of sample's visible light region is significantly greater than the other samples. Therefore, it is hypothesized that the introduction of graphene can better absorb the visible light and enhance the photocatalytic activity.

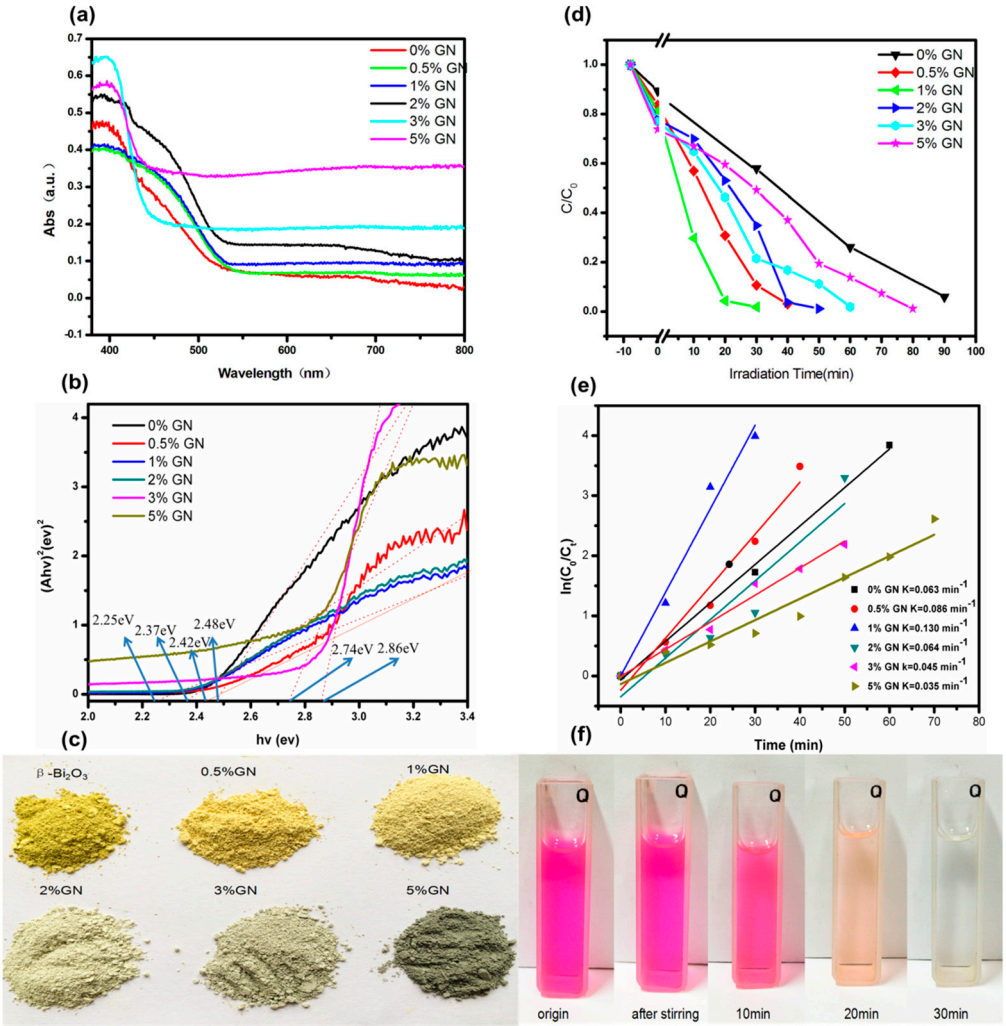

Figure 5. (**a**) The spectrogram of UV-VIS diffuse reflectance of GN with different mass ratios; and (**b**) corresponding band gap energy; (**c**) the chart of the corresponding sample color change; (**d**) the Rhodamine B (RhB) degradation rates of samples with different quantity ratios of GN; (**e**) kinetic curve of photodegradation; (**f**) color change chart of RhB solution by 1% GN degradation.

The tests of photocatalytic degradation of RhB (Figure 5d) show that all of the composites have higher degradation rates than bare β-Bi_2O_3, suggesting that there is a synergistic effect between the GN sheet and β-Bi_2O_3 nanoparticles. The sequential dye degradation rates are as follows: 1% GN > 0.5% GN > 2% GN > 3% GN > 5% GN > bare β-Bi_2O_3. It seen that only the low content (1%) of GN is introduced, the dye degradation rate can be significantly increased by three times in comparison with the bare β-Bi_2O_3. The kinetics of photodegradation reaction are investigated in Figure 5e, and the

results show that 1% GN composite has the highest constant photodegradation reaction rate, which is 0.130 min^{-1}. With the increase of GN content, the dye degradation rate did not always increase; the activity of 5% GN was significantly less than that of 1% GN. The reason why the degradation ratio decreased as the content of graphene increased was that the introduction of a large mass of black graphene would result in a rapid decrease of the light absorption of the reaction solution [23,24]. Thus, in order to achieve an optimal photocatalytic performance, it is crucial to control the composition ratio in the nanocomposite of β-Bi_2O_3/GN.

3.6. Possible Mechanisms Speculation

According to the above experimental results, the possible photocatalytic mechanisms of β-Bi_2O_3/GN were estimated, as shown in Figure 6. Under simulated sunlight irradiation, the excited electrons of the β-Bi_2O_3 semiconductor divert a part of the electrons out due to the good conductivity of the graphene layers in the course of being conducted to the conduction band. In other words, in the system of β-Bi_2O_3/GN, the graphene, as the receiving body and conductor of the electrons, effectively separated the photogenerated electron-hole pairs to avoid the recombination of electrons and holes. It's similarly compared with a previously studied system in which the GO embedded into TiO_2 nanofiber and served as a conduit of electron transfer [25]. Posa et al. [10] and Li et al. [23] prepared graphene–TiO_2 nanocomposite and CdS-cluster-decorated graphene nanosheets respectively; the similar mechanisms were proposed, too. Furthermore, the unique features of graphene also contribute to the improvement of photocatalytic activity, which allow photocatalytic reactions to take place not only on the surface of semiconductor catalysts, but also on the graphene sheet, greatly enlarging the reaction space.

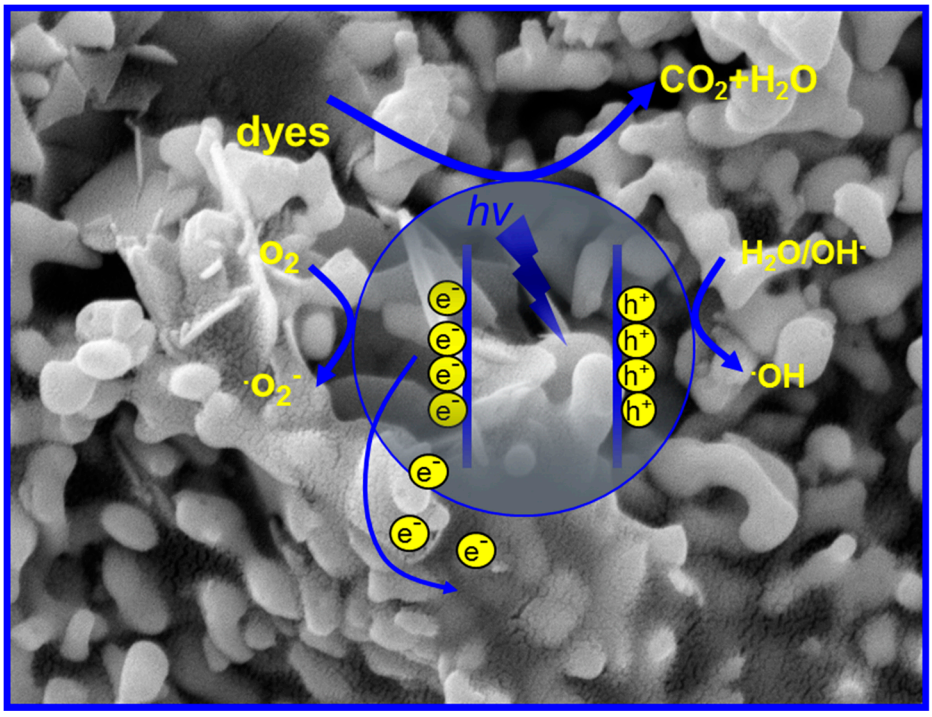

Figure 6. Speculation schematic of β-Bi_2O_3/GN photocatalytic degradation mechanism of dye.

4. Conclusions

With the simple method of solution mixing, β-Bi_2O_3/GN composite photocatalysts with different qualities were successfully prepared. In the test of degradation rate, it was found that the sample with 1% GN on its surface had the highest photocatalytic activity, with its dye degradation efficiency

being three times higher than the pure β-Bi_2O_3. However, when the content of GN increased, the degradation rate decreased. This was because the introduction of more graphene may decrease the light absorption of the reaction solution. Overall, the introduction of appropriate quantity of graphene could significantly increase the photocatalytic degradation rate of the catalyst.

Supplementary Materials: The following are available online at http://www.mdpi.com/1996-1944/11/8/1359/s1, Figure S1: The emission spectrum of a 300-W Xenon lamp (CEL-HXF300, AULTT, Beijing, China).

Author Contributions: Writing-Original Draft Preparation, J.Y. and T.X.; Writing-Review & Editing, J.Y. and T.X.; Supervision, C.L. and L.X.; Funding Acquisition, J.Y.

Funding: This research was funded by Scientific and Technological Research Program of Chongqing Municipal Education Commission (KJ1711286) and Chongqing Basic Science and Advanced Technology Research Program (CSTC2015jcyjBX0015).

Acknowledgments: We want to thank the financial support from Scientific and Technological Research Program of Chongqing Municipal Education Commission (KJ1711286) and Chongqing Basic Science and Advanced Technology Research Program (CSTC2015jcyjBX0015).

Conflicts of Interest: The authors declare no conflict of interest.

References

1. Maeder, T. Review of Bi_2O_3 based glasses for electronics and related applications. *Int. Mater. Rev.* **2013**, *58*, 3–40. [CrossRef]
2. Cabot, A.; Marsal, A.; Arbiol, J. Bi_2O_3 as a selective sensing material for NO detection. *Sens. Actuators B Chem.* **2004**, *99*, 74–89. [CrossRef]
3. Zhou, L.; Wang, W.Z.; Xu, H.L.; Sun, S.M.; Shang, M. Bi_2O_3 hierarchical nanostructures: Controllable synthesis, growth mechanism and their application in photocatalysis. *Chem. Eur. J.* **2009**, *15*, 1776–1782. [CrossRef] [PubMed]
4. Cheng, H.F.; Huang, B.B.; Lu, J.B.; Wang, Z.Y.; Xu, B.; Dai, Y. Synergistic effect of crystal and electronic structures on the visible-light-driven photocatalytic performances of Bi_2O_3 polymorphs. *Phys. Chem. Chem. Phys.* **2010**, *12*, 15468–15475. [CrossRef] [PubMed]
5. Cai, G.Y.; Xu, L.L.; Wei, B.; Che, J.X.; Gao, H.; Sun, W.J. Facile synthesis of β-Bi_2O_3/$Bi_2O_2CO_3$ nanocomposite with high visible-light photocatalytic activity. *Mater. Lett.* **2014**, *120*, 1–4. [CrossRef]
6. Li, R.H.; Chen, W.X.; Kobay, H.; Ma, C.X. Platinum-nanoparticle-loaded bismuth oxide: An efficient plasmonic photocatalyst active under visible light. *Green Chem.* **2010**, *12*, 212–215. [CrossRef]
7. Anandan, S.; Lee, G.J.; Chen, P.K.; Fan, C.; Wu, J. Removal of Orange II Dye in Water by Visible Light Assisted Photocatalytic Ozonation Using Bi_2O_3 and Au/ Bi_2O_3 Nanorods. *Ind. Eng. Chem. Res.* **2010**, *49*, 9729–9737. [CrossRef]
8. Chai, S.Y.; Kim, Y.J.; Jung, M.H.; Chakraborty, A.K.; Jung, D.; Lee, W.I. Heterojunctioned BiOCl/Bi_2O_3, a new visible light photocatalyst. *J. Catal.* **2009**, *262*, 144–149. [CrossRef]
9. Xiang, Q.; Yu, J.; Jaroniec, M. Graphene-based semiconductor photocatalysts. *Chem. Soc. Rev.* **2012**, *41*, 782–796. [CrossRef] [PubMed]
10. Posa, V.R.; Annavaram, V.; Koduru, J.R.; Bobbala, P.; Madhavi, V.; Somala, A.R. Preparation of graphene-TiO_2 nanocomposite and photocatalytic degradation of Rhodamine B under solar light irradiation. *J. Exp. Nano Sci.* **2016**, *11*, 722–736. [CrossRef]
11. Rania, S.; Aggarwal, M.; Kumarc, M.; Sharma, S.; Kumard, D. Removal of methylene blue and rhodamine B from water byzirconium oxide/graphene. *Water Sci.* **2016**, *30*, 51–60. [CrossRef]
12. Suresh, M.; Sivasamy, A. Bismuth oxide nanoparticles decorated raphene layers for the degradation of Methylene blue dye under visible light irradiations and antimicrobial activities. *J. Environ. Chem. Eng.* **2018**, *6*, 3745–3756. [CrossRef]
13. Tirtha, S.T.; Troppenz, G.V.; Wendt, R.R.; Wollgarten, M. Graphene Oxide/α-Bi_2O_3 Composites for Visible-Light Photocatalysis Chemical Catalysis and Solar Energy Conversion. *ChemSusChem* **2014**, *7*, 854–865. [CrossRef]

14. Maruthamania, D.; Vadivela, S.; Kumaravela, M.; Saravanakumarb, B.; Paulc, B.; Sankar, D.S.; Habibi-Yangjehd, A.; Manikandane, A.; Ramadoss, G. Fine cutting edge shaped Bi_2O_3 rods/reduced graphene oxide (RGO)composite for supercapacitor and visible-light photocatalytic applications. *J. Colloid Interface Sci.* **2017**, *498*, 449–459. [CrossRef]
15. Cao, S.; Chen, C.; Xie, X. Hypothermia-controlled Co-precipitation route to deposit well-dispersed β-Bi_2O_3 nanospheres on polymorphic graphene flakes. *Vacuum* **2014**, *102*, 1–4. [CrossRef]
16. Hu, X.F.; Mohamood, T.; Ma, W.H.; Chen, C.C.; Zhao, J.C. Oxidative Decomposition of Rhodamine B Dye in the Presence of VO^{2+} and/or Pt(IV) under Visible Light Irradiation: N-Deethylation, Chromophore Cleavage, and Mineralization. *J. Phys. Chem. B* **2006**, *110*, 26012–26018. [CrossRef] [PubMed]
17. Patrick, W.; Stephan, D. Photodegradation of rhodamine B in aqueous solution via SiO_2@TiO_2 nano-spheres. *J. Photochem. Photobiol. A* **2007**, *185*, 19–25. [CrossRef]
18. Daniela, C.M.; Dmitry, V.K.; Jacob, M.B.; Alexander, S.; Sun, Z.Z.; Slesarev, A.; Alemany, L.B.; Lu, W.; Tour, J.M. Improved Synthesis of Graphene Oxide. *ACS Nano* **2010**, *4*, 4806–4814. [CrossRef]
19. Adivel, S.; Keerthi, V.M.; Muthukrishnaraj, A.; Balasubramanian, N. Solvothermal synthesis of Sm-doped BiOBr/RGO composite as an efficient photocatalytic material, for methyl orange degradation. *Mater. Lett.* **2014**, *128*, 287–290. [CrossRef]
20. Lu, Y.G.; Yang, Y.C.; Ye, Z.X.; Liu, S.Y. Preparation and Visible Light Responsive Photocatalytic Activity of Nitrogen-doped Bi_2O_3 Phocatalyst. *J. Inorg. Mater.* **2012**, *6*, 643–648. [CrossRef]
21. Chi, S.; Kim, B. Nuclear Graphites (I): Oxidation Behaviors. *Carbon Lett.* **2009**, *10*, 239–249. [CrossRef]
22. Chen, C.; Long, M.; Xia, M.; Cai, W. Reduction of Graphene Oxide by An in-Situ Photoelectrochemical Method in a Dye-Sensitized Solar Cell Assembly. *Nanoscale Res. Lett.* **2012**, *7*, 1–5. [CrossRef] [PubMed]
23. Li, Q.; Guo, B.; Yu, J.; Ran, J.; Zhang, B.; Yan, H.; Gong, JR. Highly Efficient Visible-Light-Driven Photocatalytic Hydrogen Production of CdS Cluster Decorated Graphene Nanosheets. *J. Am. Chem. Soc.* **2011**, *133*, 10878–10884. [CrossRef] [PubMed]
24. Yu, J.; Ma, T.; Liu, S. Enhanced photocatalytic activity of mesoporous TiO_2 aggregates by embedding carbon nanotubes as electron-transfer channel. *Phys. Chem. Chem. Phys.* **2011**, *13*, 3491–3501. [CrossRef] [PubMed]
25. Kim, H.L.; Kim, S.; Kang, J.K.; Choi, W.Y. Graphene oxide embedded into TiO_2 nanofiber: Effective hybrid photocatalyst for solar conversion. *J. Catal.* **2014**, *309*, 49–57. [CrossRef]